3D HYDRODYNAMICAL MODELING OF CIRCULARIZATION IN BINARY SYSTEMS

F. V. Sirotkin
Astronomical observatory, Odessa National University.

ABSTRACT. Results of Three-dimensional hydrodynamical modelling of circularization process in binary systems at early stages of evolution are presented. It is shown, that circularization for systems in which the components fill their Roche lobe and are on the Hayashi track, occurs for times about hundreds of orbital periods. Thus, the binary systems such as V382 Cyg reach on the Main Sequence, having already a circular orbit.

Key words: computational fluid dynamics, binary star, circularization

Introduction

Mechanisms of a rounding off of an orbit in the binary systems of the main sequence it well studied (Zahn 1970, 1975). The basic mechanism of a rounding off of an orbit for the solar type stars ($M < 1.5-1.6M_{\odot}$) containing an extended convective envelope, is the mechanism turbulent of damping of energy of orbital motion of stars in equilibrium tides. Equilibrium tidal humps are directed not along the line of centers, and resulting not along the line of the centers, because the viscosity of substance in a stellar envelope is present. It results in transfer of the moment of rotation and energy of rotation of a star to an orbit and back. Efficiency of this mechanism strongly depends on the relation of radii of components to the size of orbital separation (characteristic time of a rounding off of an orbit $t_{circ} \sim \Big(R/A\Big)^{-8}$) (Zahn 1975). For massive stars ($M > 1.6M_{\odot}$) with radiative envelope and convective core the efficiency of a rounding off of an orbit is essentially smaller because of low viscosity of substance ($t_{circ} \sim \Big(R/A\Big)^{-10.5}$)(Zahn 1975).

Here we investigated the mechanism of rounding off of an orbit at an early stage of evolution of components of binary system, when the components on the Hayashi track, when it is possible to believe, that the stellar structure is fully convective.

SPH approximation

Here we shall give the review of the SPH method, in volume necessary for understanding of the solution. More detailed reviews are given in (Monaghan 1992, Gingold Monaghan 1977).

The equations of hydrodynamics are represented in three parts: the continuity equation

$$\frac{d\rho}{dt} = -\rho\nabla\cdot\vec{v} \tag{1}$$

the equation of energy

$$\frac{dQ}{dt} = -\frac{P}{\rho}\nabla\cdot\vec{v} \tag{2}$$

the equations of movtion.

$$\frac{d\vec{v}}{dt} = -\frac{1}{\rho}\vec{\nabla}P + \vec{F} \tag{3}$$

Here ρ is density, $\vec{v}$ is velocity, P is gas pressure. The system (1 - 3) is not complete, as the constraint equation supplementing system we have a used polytropic equation of state

$$P = K\rho^{\gamma}\ ,\ \gamma = 1 + n^{-1} \tag{4}$$

where n is polytropic index, K entropic constant. Presence of fully convective envelope allows to use for polytropic exponent the value 1.5.

Presence of viscosity, rotation and tidal deformation demands to use more general equation a state

$$P = K(S)\rho^{\gamma} \tag{5}$$

Where S entropy

$$S = (\gamma - 1)^{-1} ln\Big(\frac{P}{\rho^{\gamma}}\Big) \tag{6}$$

The equation (2) is approximate. Exact expression should contain the terms responsible the radiation and convective transfer of energy, allocation of energy in nuclear reactions, etc. But the calculations discussed

in the subsequent section concern primarily the hydrodynamics of tidal dissipation and ignore such issues as radiation transport and pressure thermonuclear of burn or complications due to magnetic fields. Radiation process can reasonably ignored because the diffusion time scale are quite long compared with the dynamic time scale for circularization in considered systems.

The core of SPH is an interpolation method which allows any function to be expressed in terms of its values at set of disordered points-the particles. Any quantity can be determined as

$$A_s(\vec{r}) = \int A(r')W(r-r',h)dr' \tag{7}$$

Where integration is made on all volume, and $W(r,h)$ is kernel which satisfying conditions:

$$\int W(r-r',h)dr' = 1 \tag{8}$$

$$\lim_{h\to 0} W(r-r',h) = \delta(r-r') \tag{9}$$

For numerical work, the integral (7) can be approximate by a summation.

$$A_s(\vec{r}) = \sum_{i=1}^{N}\left[\frac{A(\vec{r_i})}{\rho(\vec{r_i})}\right]W(|\vec{r}-\vec{r}_i|,h) \tag{10}$$

The variable h in SPH has the same sense, as in finite-difference methods the size of a grid. Using SPH we can write the continuity equation such as

$$\rho(\vec{r}) = \sum_{i=1}^{N} m_i W(|\vec{r}-\vec{r}_i|,h) \tag{11}$$

or

$$\frac{d\rho(\vec{r})}{dt} = \sum_{i=1}^{N} m_i(\vec{v}-\vec{v}_i)\cdot\nabla W(|\vec{r}-\vec{r}_i|,h) \tag{12}$$

In our work, we have used the equation (11), because it equation guarantees conservation of mass The momentum equation

$$\frac{d\vec{v}_i}{dt} = -\sum_{j=1}^{N} m_j\left(\frac{P_i}{\rho_i^2}+\frac{P_j}{\rho_j^2}\right)\cdot\nabla W(|\vec{r}_i-\vec{r}_j|,h) - G\sum_{j=1}^{N}\frac{M(r_{ij})}{r_{ij}^2}\hat{r}_{ij} + \vec{F}_{visc,i} \tag{13}$$

The first terms in the right part of expression (13) it SPH approximation of a gradient of gas pressure. The second term is a gravity action on a particle in a point $\vec{r}_i$ on the part of other particles. Here $M(r_{ij})$ weight of matter inside sphere with the center in $\vec{r}_i$ and radius r_{ij}:

$$r_{ij} = |\vec{r}_i - \vec{r}_j|\ ,\ \hat{r}_{ij} = \frac{\vec{r}_i-\vec{r}_j}{r_{ij}}$$

$$M(r_{ij}) = 4\pi\int_0^{r_{ij}} r^2\rho(r)dr = 4\pi m_i\int_0^{r_{ij}} r^2 W(r,h)dr$$

The third term in the right part of expression (13) is accounts for viscosity forces. At numerical modelling, as a rule, an artificial viscosity is added. We have used the following form of artificial viscosity (Monaghan ,1992):

$$\vec{F}_{visc,i} = \sum_{j=1}^{N}\Pi_{ij}m_j\nabla_i W(r_{ij},h)dr \tag{14}$$

$$\begin{cases} \Pi_{ij} = -\dfrac{\alpha\mu_{ij}c_{ij}+\beta\mu_{ij}^2}{\rho_{ij}} & ,\quad (\vec{v}_i-\vec{v}_j)\cdot(\vec{r}_i-\vec{r}_j) > 0 \\ \Pi_{ij} = 0 & ,\quad (\vec{v}_i-\vec{v}_j)\cdot(\vec{r}_i-\vec{r}_j) < 0 \end{cases}$$

$$\mu_{ij} = \frac{h(\vec{v}_i-\vec{v}_j)\cdot(\vec{r}_i-\vec{r}_j)}{r_{ij}^2+\varepsilon^2 h} \tag{15}$$

$$c_{ij} = 0.5(c_i+c_j) \quad \rho_{ij} = 0.5(\rho_i+\rho_j)$$

Here c_i is a sound speed at a point $\vec{r}_i$, α,β,ε are constants selected by the decision of standard modelling tasks (Monaghan ,1992). In our work $\alpha = 0.5, \beta = 1$. The parameter ε is put into equation (15) to prevents singularities. This form of artificial viscosity has a number of desirable features (Monaghan ,1992):

1. it is Galilean invariant
2. it vanishes for rigid body rotation
3. it conserves total linear and angular momenta.

SPH approximation of the equation of energy looks like (Hernquist , 1993)

$$\frac{dK_i}{dt} = \frac{\gamma-1}{2\rho_i^{\gamma-1}}\sum_{j=1}^{N}\Pi_{ij}m_j(\vec{v}_i-\vec{v}_j)\cdot\nabla_i W_{ij} \tag{16}$$

The use of different kernels is the SPH is analogue of the use of different difference schemes in finite difference methods. We use the Gaussian kernel, because with this kernel, SPH equations has a simplest physical interpretation. In addition, SPH expressions received with Gaussian kernel have higher accuracy in

comparison with expressions based on splines (Monaghan ,1992).

$$W(r,h) = \frac{\exp(-\frac{r^2}{h^2})}{\pi^{3/2}h^3} \tag{17}$$

Then, the system which we should solve can be written down as:

$$\begin{aligned}
\rho_i &= \sum_{j=1}^{N} m_j W(r_{ij},h) \\
\frac{d\vec{v}_i}{dt} &= -\sum_{j=1}^{N} m_j \left(\frac{P_i}{\rho_i^2}+\frac{P_j}{\rho_j^2}\right)\cdot\nabla W(|\vec{r}_i-\vec{r}_j|,h) \\
&\quad -G\sum_{j=1}^{N}\frac{M(r_{ij})}{r_{ij}^2}\hat{r}_{ij}+\vec{F}_{visc,i} \\
\frac{dK_i}{dt} &= \frac{\gamma-1}{2\rho_i^{\gamma-1}}\sum_{j=1}^{N}\Pi_{ij}m_j(\vec{v}_i-\vec{v}_j)\cdot\nabla_i W_{ij} \\
P_i &= K_i\rho_i^{\gamma}
\end{aligned} \tag{18}$$

Time step. Courant - Levy condition

In this, we applied to SPH more popular integration schemes - predictor-corrector scheme,the following equations are used to obtain the field quantities at next time step.

$$\begin{aligned}
\tilde{v}^{1/2} &= v^0+\tfrac{\Delta t}{2}f^0 \\
\tilde{r}^{1/2} &= r^0+\tfrac{\Delta t}{2}v^0 \\
\rho^{1/2} &= \rho(r^{1/2}) \\
f^{1/2} &= f(r^{1/2},\rho^{1/2},v^{1/2},...) \\
v^{1/2} &= v^0+\tfrac{\Delta t}{2}f^{1/2} \\
r^{1/2} &= r^0+\tfrac{\Delta t}{2}v^{1/2} \\
r^1 &= 2r^{1/2}-r^0 \\
v^1 &= 2v^{1/2}-v^0
\end{aligned} \tag{19}$$

Here, the superscripts refer to time step index, and f the force per unit mass (acceleration). The time step should be chosen to accommodate the Courant-Levy condition, which, essentially, states that the maximum rate of propagation of information numerically must exceed the physical rate. In SPH, this translates to

$$\frac{h}{\Delta t} \geq c_s \tag{20}$$

where c_s is the sound speed. Because the viscosity is present, it should be also be taken into account:

$$\Delta t_2 = \min_i\Big(\frac{h_i}{c_i+\alpha c_i+\beta\max_i|\mu_{ij}|}\Big) \tag{21}$$

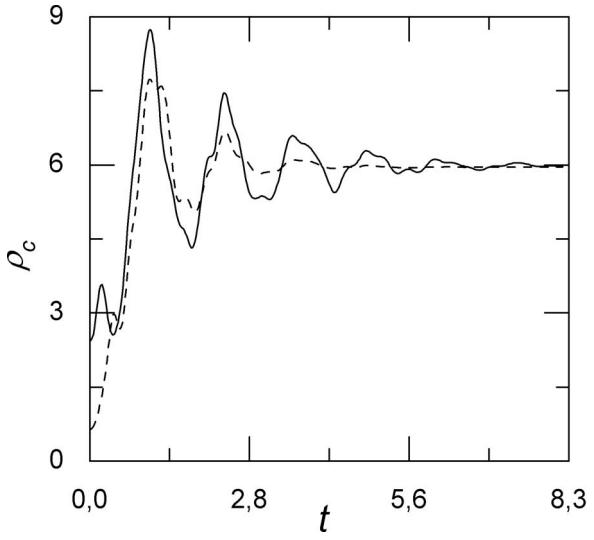

Figure 1: The central density ρ_c as a function time t for two dumped hydrodynamic sequences with equivalent initial conditions and different dumping constant.

to ensure that the forces exerted on individual particles are integrated correctly, the time step should also be less then

$$\Delta t_1 = \min_i\Big(\frac{h_i}{f_i}\Big)^{1/2} \tag{22}$$

here f_i force per unit mass. So, a suitable time step for the scheme is

$$\Delta t = C_N\min(\Delta t_1,\Delta t_2) \tag{23}$$

Model of a single polytropic star.

A smoothing length h

The decision of the primary goal demands to assign the boundary conditions for system (18), besides this, result of SPH approximation respects depends on size of h. Calculation of model a single polytropic star taking place in a condition of hydrostatic balance and comparison of the received result with results the received other methods allows to find a boundary conditions and sizes of the h.

To construct a static model we follow the dumped motion of a set of particles from some initial distribution of position until system comes to rest. Particles were initially at rest, distributed in space either according to random Gaussian distribution (see Fig.13, Fig.14). For this case, it is possible to write down sys-

tem (18) as (Gingold , Monaghan,1977)

$$\rho_i = \sum_{j=1}^{N} m_j W(r_{ij}, h)$$

$$P_i = K\rho_i^{\gamma} \quad (24)$$

$$\frac{d\vec{v_i}}{dt} = -\Gamma\frac{d\vec{r}_i}{dt} - K\gamma\rho_i^{\gamma-2}\nabla\rho - G\sum_{j=1}^{N}\frac{M(r_{ij})}{r_{ij}^2}\hat{r}_{ij}$$

Here there is no expression for polytropic temperature because the it is constant for all star (Chandrasekhar ,1950)

$$K = N_n\ G\ M^{2-\gamma}\ R^{3\gamma-4} \quad (25)$$

Here R radius and M is mass of the star.

The approach to equilibrium for two initial configuration with different dumping constant satisfying conditions $0 < \Gamma < 1$ is illustrated in Fig. 1 for polytropic index $n = 1.5$. The solid line represents the behavior of central density ρ_c as a function of the time t, in a sequence that commences with 1000 particles distributed in space either according to random Gaussian distribution and $\Gamma = 0.98$. The broken curve shows a sequence with $\Gamma = 0.95$.

Value of a spatially resolution h on each step of integration was from this condition:

on first step

$$h^0 = \frac{R}{N^{1/3}} \quad d^0 = \frac{h^0}{2}$$

on $s+1$ step

$$h^{s+1} = h^s + d^s \quad \rho_c^s > \rho_t$$

$$h^{s+1} = h^s - d^s \quad \rho_c^s < \rho_t$$

$$d^{s+1} = \frac{d^s}{2}$$

Here ρ_t is central density designed by others method (for example SCF method give for polytropic index $n = 1.5$ value of ρ_t is 5.99071). For example, for a star with $M = M_\odot$, $R = R_\odot$ and $N = 1000$ value of a spatially resolution h is $0.1105R_\odot$. Final distribution of particles is submitted in figures Fig. 15 and Fig. 16

Initial conditions. Data structure

As a result of construction of polytrope model by a method described in the previous paragraph we shall define distribution of particles corresponding to hydrostatic. Transition to system of coordinates connected with the center of weights of the binary system gives for the first component

$$\vec{v}_i = k_\omega\vec{\Omega}\times\vec{r}_i + k_\omega\vec{\Omega}\times\vec{r}_c,\ i = 1...N$$

$$\vec{r}_i = \vec{r}_i + \vec{r}_c$$

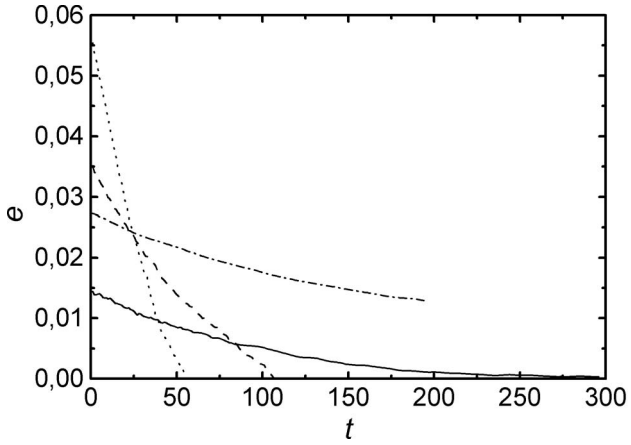

Figure 2: The eccentricity as a function time. Sold line $k_\omega = 1$, dotted $k_\omega = 0.98$, dashed $k_\omega = 0.99$, dash-dotted $k_\omega = 1.02$

for the second component

$$\vec{v}_i = k_\omega\vec{\Omega}\times\vec{r}_i - k_\omega\vec{\Omega}\times\vec{r}_c,\ i = N+1..2N$$

$$\vec{r}_i = \vec{r}_i - \vec{r}_c$$

where $\vec{r_c}$ is a vector of position of the center of weights of system, k_ω any factor. The $\vec{\Omega}$ is an angular velocity corresponding to the Kepler's third law which is not obliged to be carried out for a case of not point mass.

For each star we use an equal number of particles and an equal polytropic index. For all models $M_1 = 27.2M_\odot$(primary component), $M_2 = 19.25M_\odot$ (secondary component) , $R_1 = 9.45R_\odot$, $R_2 = 8.5R_\odot$, $N = 2000$ (1000 per star), $n = 1.5$, initial orbital separation $A_0 = 26R_\odot$ (Fig.9 initial density distribution for all models). We change the parameter k_ω from model to model. Thus, we limit quantity of varied parameters in view of complexity of the decision of a problem completely.

Results

The factor k_ω varied in limits from 0.96 up to 1.04. The time step made $\sim 1\%$ from an initial period. In total it has been constructed ten models.

- For values $0.96 < k_\omega < 0.995$ as a result of a transient mass transfer (Fig.11 Fig.12) there is an increase of orbital separation. It is interesting to note, that an interval of values k_ω at which it to occur narrow. calculation were not made after the moment of the termination of a mass transfer.
- For values $0.995 < k_\omega < 1.016$ there is a rounding off of an orbit to value of final orbital separation less initial.

- For values $k_\omega > 1.016$ there is a rounding off of an orbit to value of final orbital separation more initial. Its is difficult to determine precisely the circularization time, because of huge amount of computational time.

The analysis of time variability of orbital angular moment in (Fig.8) shows, that, for all models on a curve it is possible to allocate two basic stages. On an initial stage there is practically linear decrease or increase of the angular moment (Fig.5 dashed line) and further there is a sharp change of character of behavior of a curve. For values $0.96 < k_\omega < 0.995$ at which there is mass transfer, it corresponds to the beginning of an exchange in mass. Further, there are probably two variants of evolution, for systems with $k_\omega < 0.995$ there is a fast reduction of size of the angular moment. For systems with $k_\omega > 0.995$ the further change of the orbital angular moment looks as fading periodic fluctuations concerning a horizontal site (Fig.5 dotted line). For all models, the full angular momentum is strictly conserved.

In behavior of other characteristics of components of binary system there are same features, as at behavior of the orbital angular moment (Fig.5, Fig.4, Fig.3, Fig.7).

For any values of k_ω eccentricity decreases (Fig.2). Time of a rounding off strongly depends on the relation of radii of components to size of orbital separation in periastron. On the other hand, the size of orbital separation in periastron depends on k_ω (from a condition of a task). Dependence of circularization time on k_ω can be approximated the following formula (Fig.6):

$$t_{circ} = \exp(-1488.36 + 2896.74k_\omega - 1402.39k_\omega^2) \pm 18.81 \quad (26)$$

The obtained circularization times are insignificant in comparison to circularization time for stars at Main Sequence. It can serve as an argument for the benefit of the assumption that circularization can occur at early stages of evolution of closed binary stars, and as a result they can get on the main sequence, having already circular orbits.

Acknowledgements The author is thankful to I.L.Andronov and V.G.Karetnikov for valuable discussions.

References

Chandrasekhar S.: 1950. *An introduction to the study of stellar structure.* Moscow, p.135.

Cherepachuk A.M., Karetnikov V.G.: 2003, *AZh,* **80**, 42

Gingold R. A., Monaghan J.J.: 1977, *M.N.R.A.S.,* **181**, 375

Hernquist L.: 1993, *ApJ*, **404**, 717

Monaghan J. J.: 1992, *A.R.A.A.* **30**, 543

Zahn J.P.: 1970, *As.Ap.,* **4**, 452

Zahn J.P.: 1975, *As.Ap.,* **41**, 429

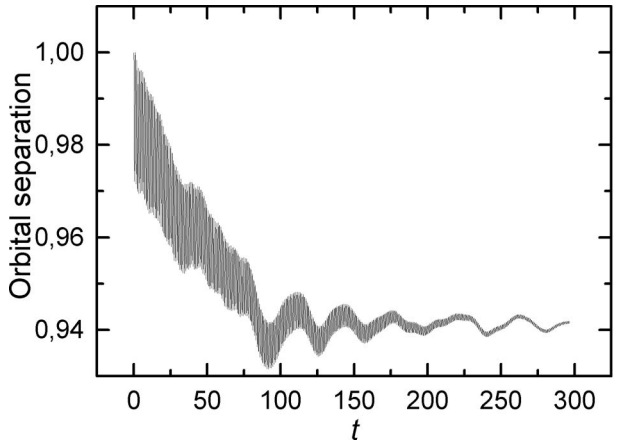

Figure 3: The orbital separation as a function of time, $k_\omega = 1$. Orbital separation is given in terms of initial orbital separation, time is given in terms of initial period

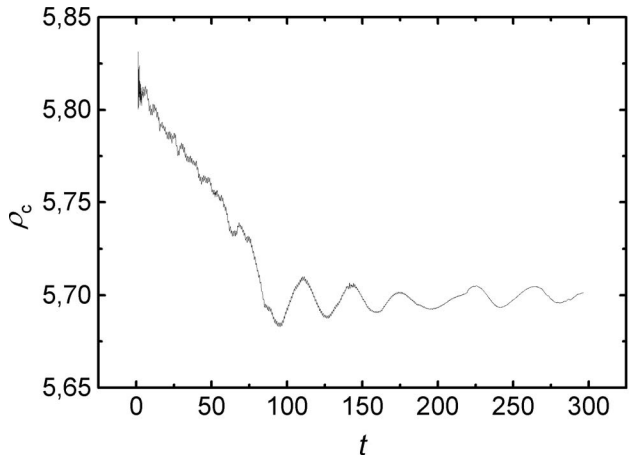

Figure 4: The central density of primary component as a function time, $k_\omega = 1$.The central density is given in terms of medium density of primary component.

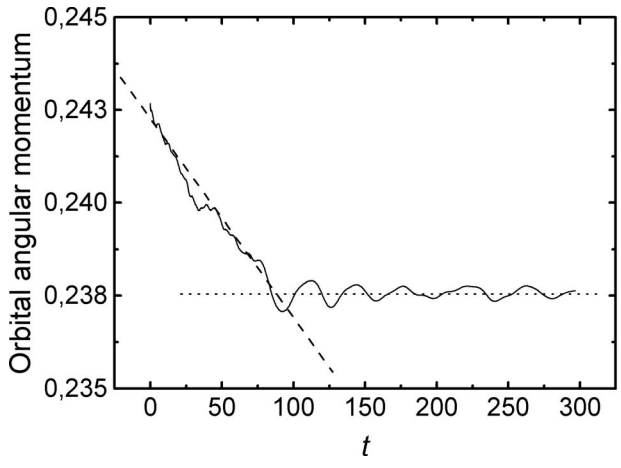

Figure 5: The orbital angular momentum as a function time, $k_\omega = 1$.

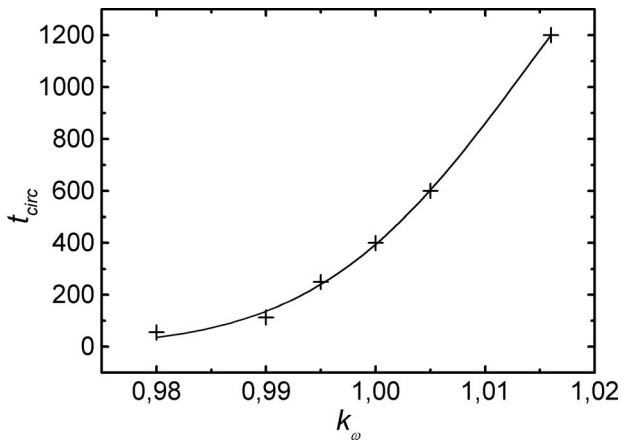

Figure 6: Circularization time as a function of k_ω.

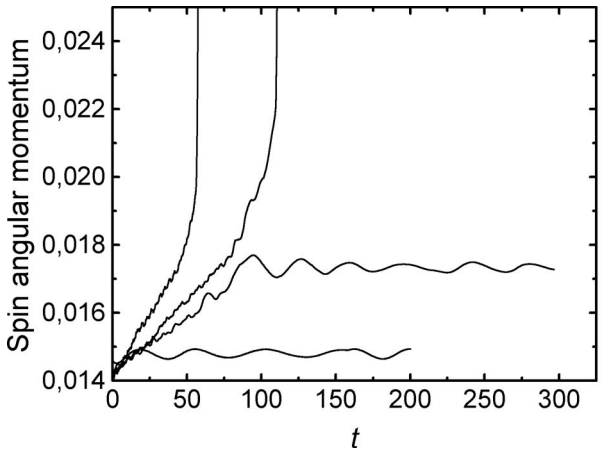

Figure 7: The spin angular momentum of primary component momentum as a function of time.

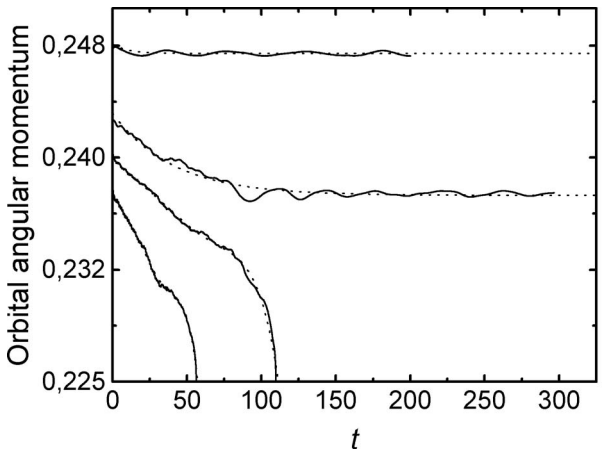

Figure 8: The orbital angular momentum as a function time. The angular momentum is given in terms $A_0^2(M_1 + M_2)/|\vec{\Omega}|$

.

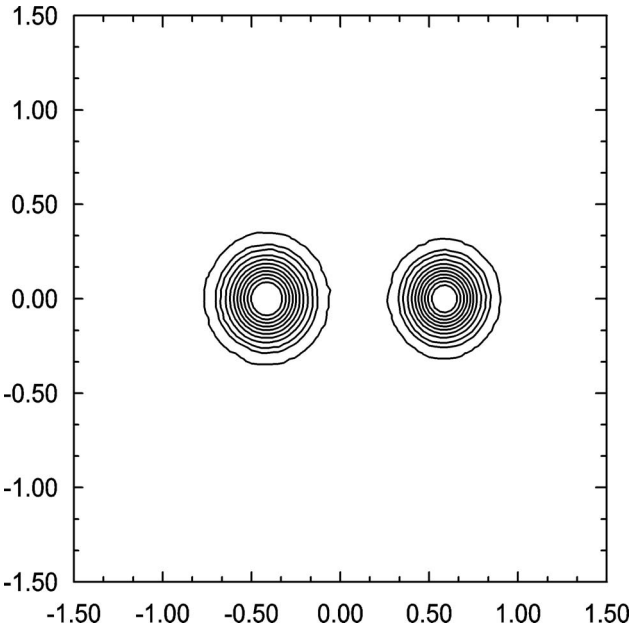

Figure 9: $t = 0$. Initial density distribution for all models. Distances are given in terms of orbital separation.

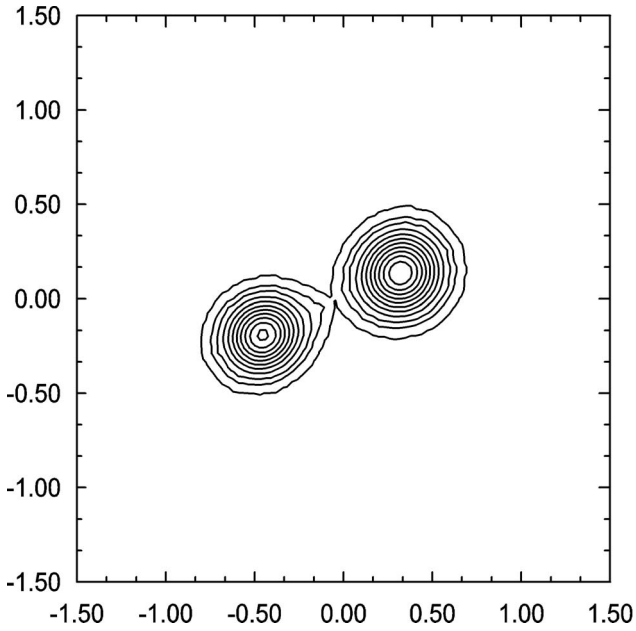

Figure 11: The beginning of mass transferring $t = 108$, $k_\omega = 0.99$

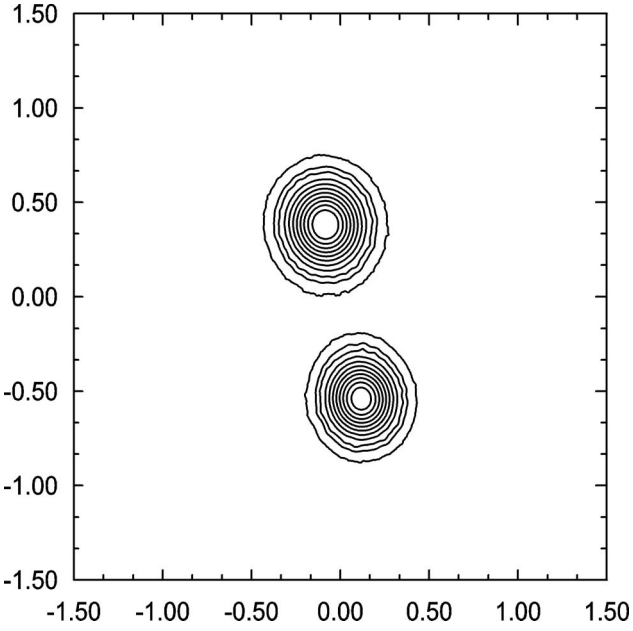

Figure 10: The final density distribution for $k_\omega = 1$, $t = 296$.

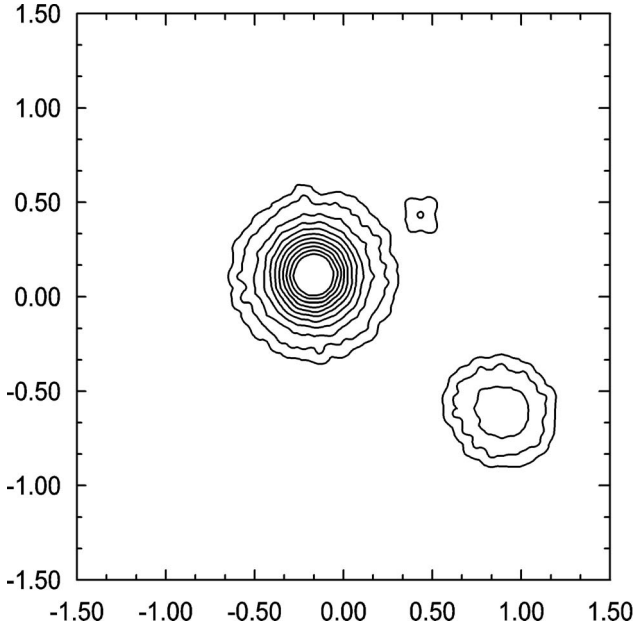

Figure 12: The final density distribution for $k_\omega = 0.99$, $t = 132$.

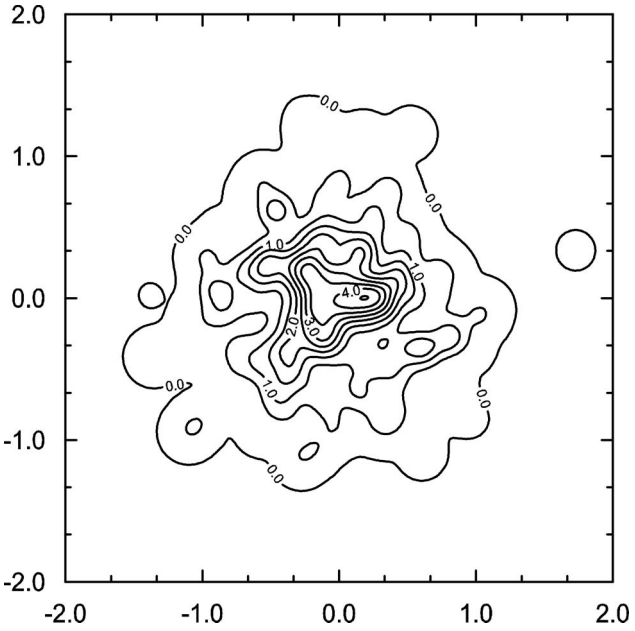

Figure 13: The initial density distribution corresponding to initial distribution of particles(bottom Figure). Density is given in terms of medium density.

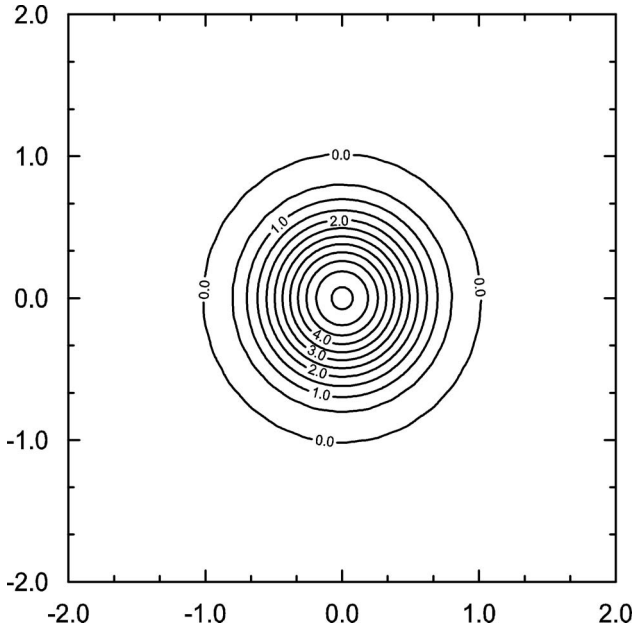

Figure 15: The final density distribution corresponding to final distribution of particles.

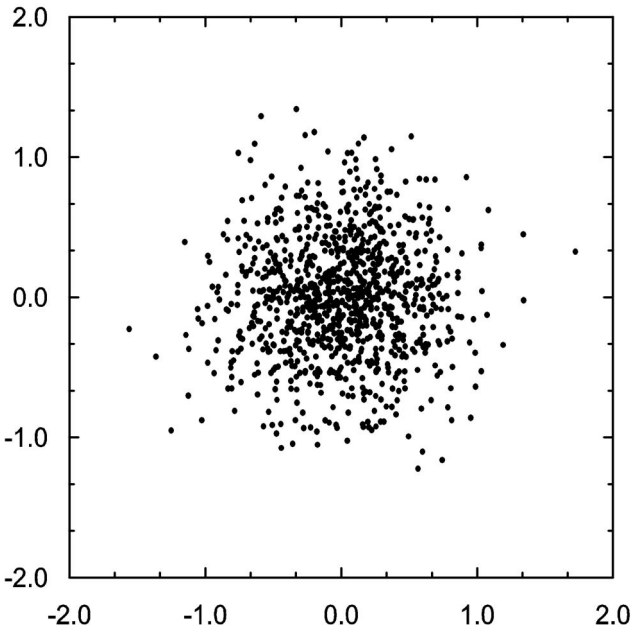

Figure 14: The initial distribution of a particles. Distances are given in terms of $R_\odot$.

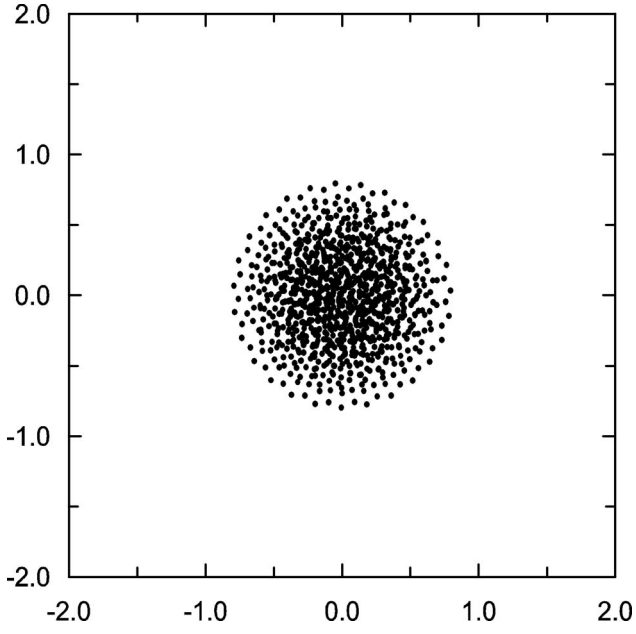

Figure 16: The final distribution of a particles. $M = M_\odot$, $R = R_\odot$, $h = 0.1105 R_\odot$